Geophysical Research Letters

RESEARCH LETTER
10.1029/2021GL096900

Key Points:

- We show that PKP precursors and PdP reflections can be produced by the same heterogeneity structure in the lowermost mantle (D″ layer)
- Our heterogeneity models consist of scatterers of different correlation lengths (10, 50 km) and velocity perturbations (1%, 3%, 5%)
- Best fitting model for PKP precursors that also generates PdP reflections has a correlation length of 10 km and velocity changes of 5%

Supporting Information:

Supporting Information may be found in the online version of this article.

Correspondence to:

V. Hiemer,
hiemer@uni-muenster.de

Citation:

Hiemer, V., & Thomas, C. (2022). Generation of reflections and PKP precursors from a scattering layer in D″. *Geophysical Research Letters*, *49*, e2021GL096900. https://doi.org/10.1029/2021GL096900

Received 4 NOV 2021
Accepted 4 FEB 2022

Generation of Reflections and PKP Precursors From a Scattering Layer in D″

Vanessa Hiemer[1] **and Christine Thomas**[1]

[1]Institut für Geophysik, Westfälische Wilhelms-Universität Münster, Münster, Germany

Abstract The D″ region consists of many different structures on many length-scales and here we test whether an inhomogeneous scattering region could potentially explain two of these seismic observables, namely PKP precursors, which are generated by scattering near the core-mantle boundary, and reflections of a seismic discontinuity in the lowermost mantle. The focus of this study is on modeling PKP precursors and lower mantle reflections. Testing different heterogeneity models with a range of correlation lengths and velocity perturbations for D″, we find that some of our models can produce both waves. Comparing our synthetic seismograms to real data for precursors in adjacent locations beneath the mid-Atlantic near South America we find the best fitting model with correlation length of 10 km and velocity perturbation of 5% with a gradual increase of scattering defined by a taper from 200 to 400 km above the core-mantle boundary.

Plain Language Summary The lowest 300 km of the Earth's mantle (called D″ layer) consists of many different structures that range from small-scale features such as scatterers to large-scale structures such as large regions with lower seismic velocity than the surrounding mantle. The structures are visible with a range of seismic waves but many studies are restricted to only one wavetype. In this study, we focus on two seismic waves that are usually associated with different structures. First, PKP precursors that are P waves scattered at small-scale features in the lowermost mantle and second the PdP wave that reflects off the D″ boundary which is associated with a sharp velocity change. We compute synthetic seismic data assuming a scattering region in D″, testing models of different scatterer sizes and strength and find that some of these models can in fact produce both wavetypes. Additionally, we find a best fitting model by comparing the synthetics with real earthquake data imaging the lower mantle beneath the mid-Atlantic near South America. We thereby show that perhaps some structures in the lowermost mantle, previously interpreted as different features, are in fact related. This may help to improve our knowledge of the geodynamical processes in the lower mantle.

1. Introduction

The Earth's mantle above the core-mantle boundary (CMB) is characterized by a variety of seismically visible structures at many different length-scales, ranging from small-scale features such as scatterers (e.g., Mancinelli et al., 2016) to large-scale structures such as large low seismic velocity provinces (LLSVP), visible in tomographic inversions (e.g., French & Romanowicz, 2015; Ritsema et al., 2011). The D″ layer (Bullen, 1949), defined as the lowest 200–300 km of the mantle, is considered to be a thermochemical boundary layer (e.g., Lay et al., 1998; Lay, 2015) and studies focusing on this layer have detected signals indicating a variety of different structures, such as ultralow velocity zones (ULVZ; e.g., Garnero et al., 1998; McNamara et al., 2010; Rost et al., 2005), subducted slabs (e.g., Davies & Gurnis, 1986; Hutko et al., 2006), scatterers (e.g., Bataille et al., 1990; Mancinelli et al., 2016), LLSVPs (e.g., Garnero et al., 2016; Koelemeijer, 2021; McNamara, 2019), and seismic anisotropy (e.g., Kendall, 2000; Maupin, 1994; Nowacki et al., 2011). In short, the CMB region and D″ layer seem to be as heterogeneous as the lithosphere with strong variations on all length-scales.

The different structures in the D″ region are detected using a range of different methods, seismic waves and source-receiver combinations. For example, to investigate scatterers in D″, mostly PKP precursors have been used (e.g., Cleary & Haddon, 1972; Hedlin & Shearer, 2000) while, for example, D″ anisotropy is often tested with splitting of S-waves (e.g., Nowacki et al., 2011) and ultra-low velocity zones (ULVZs) have been detected with so-called SPdiffKS waves (e.g., Garnero et al., 1998; Thorne et al., 2020). While the different waves indicate the presence of one type of structure, it is possible that due to interrogating with different frequencies, ray angles, and seismic wave resolution, one might actually test the same structure but due to the lack of more information one might derive an incomplete picture of the structure and therefore interpret the results differently. To

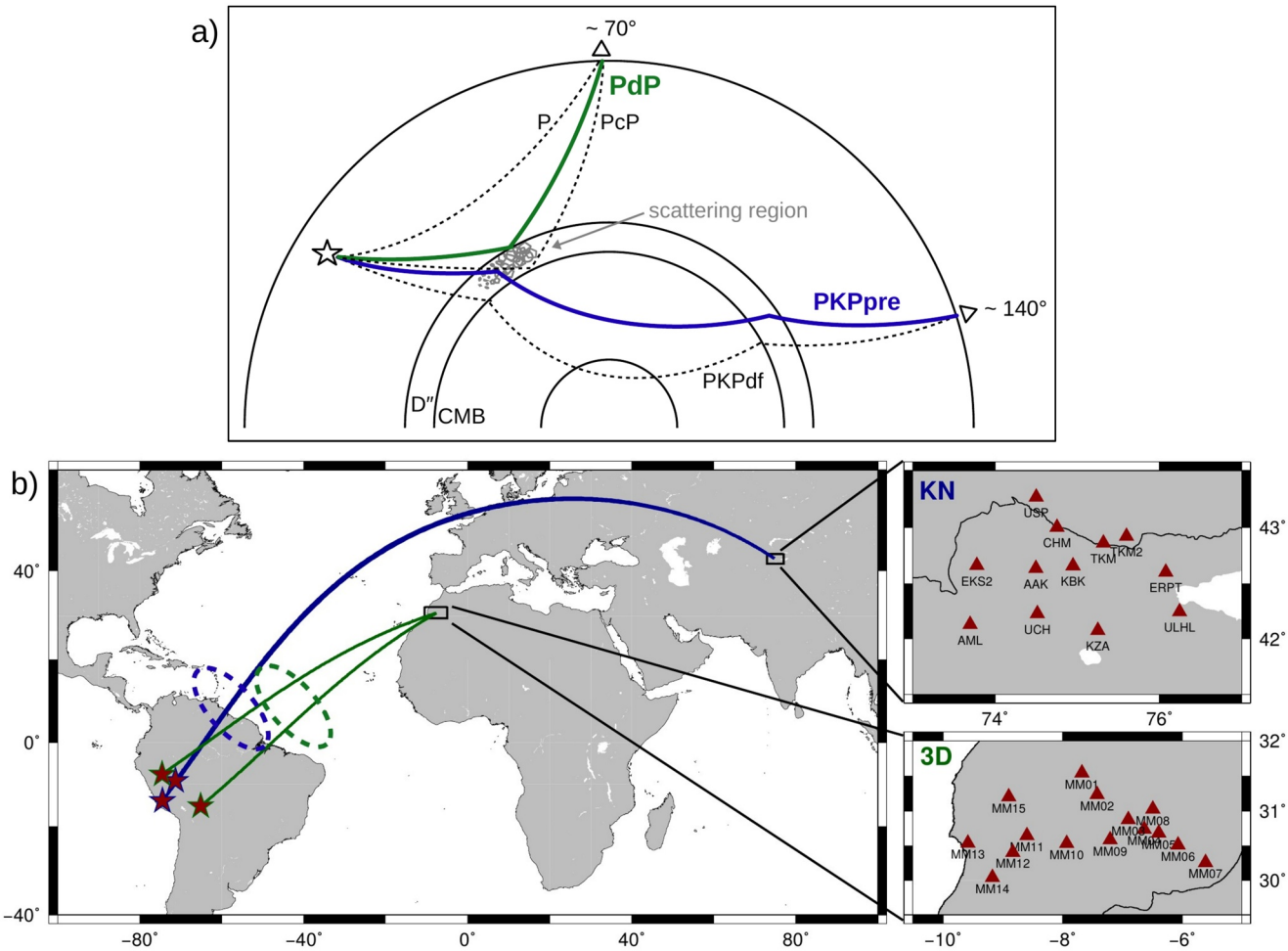

Figure 1. (a) Schematic representation of ray paths of PKP precursors (PKPpre, blue line), PKPdf as well as P-waves, PcP and PdP reflections (green line). The gray area denotes the scattering region, the star indicates the source while triangles show the receivers in 70° and 140° (CMB: core-mantle boundary). (b) Source-receiver combinations of the events shown in this study. The PKP precursors (blue great circle paths) were recorded at KN, the PdP reflections (green great circle paths) at the Münster-Morocco array (Tables S1 and S2 in Supporting Information S1). The stars represent the epicenters of the events shown in this study, the triangles indicate the location of the stations. The blue and green dashed circles represent the areas of the PKP precursor pierce points and the PdP bounce point region, respectively. They were approximated with regard to our detections of precursors and reflections in the data.

understand whether this is a possibility, here we focus on precursors to PKPdf and the PdP reflections (Figure 1) to understand whether the same structure could generate both wavetypes. PKP precursors have been shown to be generated from scattering at small-scale heterogeneities in the lower(most) mantle, while it is commonly assumed that PdP and SdS waves result from a reflection of a P- or S-wave at the D″ discontinuity. Below we will provide more information on both wave types and how they have been used.

Short-period precursors that arrive before the PKPdf phase originate from scattering of PKPab and PKPbc in the lower mantle and arrive at distances of about 120–145° (Figure 1a). The precursors were first observed by Gutenberg and Richter (1934) and first interpreted as a result from scattering of PKP waves in the lowermost mantle by Haddon (1972). Since then, many studies confirmed lowermost mantle scattering as cause for PKP precursors (e.g., Cao & Romanowicz, 2007; Doornbos, 1976; King et al., 1974; Thomas et al., 1999; Vanacore et al., 2010; Vidale & Hedlin, 1998; Waszek et al., 2015) but there are also other interpretations about the origin of PKP precursors, such as scattering in the whole or lowest 1,000 km of the mantle (e.g., Cormier, 1999; Doornbos & Vlaar, 1973; Hedlin et al., 1997; Margerin & Nolet, 2003; Mancinelli & Shearer, 2013) and scattering at CMB topography (e.g., Ansell, 1973; Bataille & Flatté, 1988; Haddon & Cleary, 1974). Recently, it has also been suggested that coherent PKP precursors could be scattered at small-scale ULVZs (Ma & Thomas, 2020), therefore connecting two of the lowermost mantle structures. Previous studies (e.g., Hedlin & Shearer, 2000; Vidale

& Hedlin, 1998; Waszek et al., 2015) suggested that small-scale scatterers may also be related to partial melt pockets or subducted slab material.

Seismic reflections from the top of the D″ region (Figure 1a) were first reported by Lay and Helmberger (1983) for S waves and by Wright et al. (1985) for P waves. The reflections are best detected between 60 and 80° epicentral distance (e.g., Cobden et al., 2015; Wysession et al., 1998) and for these distances arrive between the direct wave (P or S) and the core reflection (PcP or ScS). The reflections have initially been interpreted as originating from a velocity increase across the D″ discontinuity and this increase of P and S wave velocities at the top of D″ was subsequently the focus of many studies (e.g., Avants et al., 2006; Houard & Nataf, 1993; Hutko et al., 2008; Lay et al., 1997; Reasoner & Revenaugh, 1999; Thomas & Weber, 1997; Thomas, Garnero, & Lay, 2004; Thomas, Kendall, & Lowman, 2004; Weber & Davis, 1990). Interpretations invoked different mechanisms, such as reflection off a phase change such as bridgmanite to its high-pressure phase post-perovskite (e.g., Sidorin et al., 1999; Hernlund et al., 2005; Bower et al., 2013; Cobden et al., 2015; Lay, 2015), a reflection at subducted lithosphere (e.g., Lay & Garnero, 2004; Thomas, Garnero, & Lay, 2004; Thomas, Kendall, & Lowman, 2004; Hutko et al., 2006) or due to scattering related to subducted slabs (e.g., Scherbaum et al., 1997). However, D″ reflections have been detected also in regions without past subduction and therefore a different mechanism might cause the reflections in these areas (see reviews by e.g., Wysession et al., 1998; Cobden et al., 2015; Jackson & Thomas, 2021). In addition, some regions do not seem to generate D″ reflected waves, therefore the D″ reflector might not exist in all places (e.g., Sun et al., 2016).

In this study we concentrate on the mid-Atlantic, near the north-eastern part of South America. In this region, Weber and Körnig (1992) predicted the D″ discontinuity at 260–310 km above the CMB and found that the reflected PdP waves require a P-wave velocity contrast of 2%–3%. Pisconti et al. (2019) imaged the D″ reflector and shear wave splitting in this region. PKP precursors from this region have only been shown in global studies (Ma & Thomas, 2020; Mancinelli et al., 2016) but to our knowledge no regional studies of PKP precursors exist for this part of the Atlantic. While we will present data examples imaging the region beneath the Central Atlantic, the focus of this study is on testing whether these observations can be generated with one mechanism, therefore synthetic data are generated and analyzed.

2. Data

As part of this study we sampled the lowermost mantle with events that occurred in the western part of South America and were recorded at the Kyrgyz Seismic Network (KN) in Kyrgyzstan (Mellors, 1995; Vernon, 1992, 1998) in order to search for scattering that results in PKP precursors. In addition, and in order to sample a similar region, South American events recorded at the Münster-Morocco-Array (Spieker et al., 2014) were analyzed to search for D″ reflections (Figure 1b). Source-receiver combinations that sample the same area with PdP waves and PKP precursor waves were not found. We show two events for each wavetype (Figure 2) and their paths as well as the region where they sample the lowermost mantle at the source side are shown in Figure 1b.

We chose a distance range of 120°–145° for the search for PKP precursors and 50°–95° for PdP reflections. In agreement with previous studies, short-period filters around 1 Hz were best suited to detect the PKP precursor waves and on the other hand periods from 1 to 10 s were useful for detecting PdP waves. In Figures 2a and 2b, we show two events with good PKP precursor waves in a distance-dependent seismogram. The event in Figure 2a shows a coherent precursor while in the event in Figure 2b, the precursor energy is smaller than in Figure 2a and does not show clear coherent precursor energy.

Searching for reflections, stacking of traces is usually necessary to detect and distinguish the PdP or SdS waves from other arrivals (e.g., Cobden & Thomas, 2013; Weber, 1993) since PdP arrivals are usually small (e.g., Figure S1a in Supporting Information S1). Therefore, we use array techniques and generate vespagrams (e.g., Rost & Thomas, 2002; Schweitzer et al., 2012). Figures 2c and 2d shows two events with PdP waves in a vespagram. The PdP arrivals are visible, however, they are partly embedded in additional arrivals such as crustal reverberations, recognizable by the slowness close to P-slowness, and also noise. Also, the amplitude of PcP compared with the direct P wave differs between the two events shown in Figures 2c and 2d.

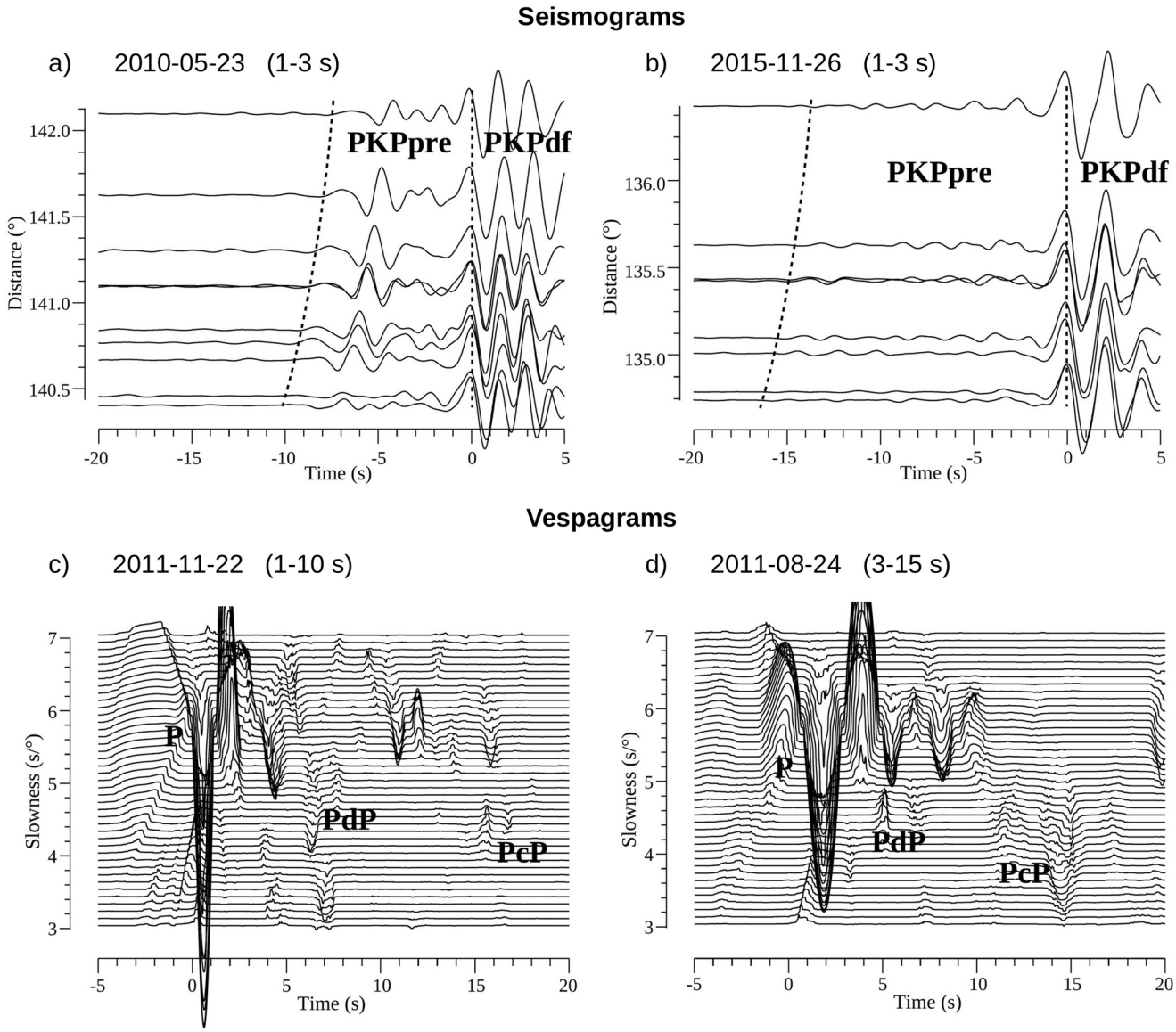

Figure 2. Data examples of PKP precursors (shown in a distance-dependent seismogram section) and PdP reflections (shown in a vespagram). (a) PKP precursor waves for the event 23 May 2010 recorded at a distance of approximately 141.1°. Dashed lines indicate arrivals of PKP and the earliest arrivals of precursors (PKPpre) (b) as (a) but for the event 26 November 2015 recorded at a distance of approximately 135.3°. (c) Vespagram of a PdP reflection for the event 22 November 2011 recorded at a distance of approximately 71.8°. The arrivals of P, PdP and PcP are shown. (d) Same as (c) but for the event 24 August 2011 recorded at a distance of approximately 74.5°. For all examples the used filter is provided.

For the following modeling we have chosen one of our precursor events (23 May 2010 in Figure 2a) and one reflection event (22 November 2011 in Figure 2c). The details of the events are given in Table S1 in Supporting Information S1.

3. Modeling of PKP Precursors and PdP Reflections, and Results

Our aim is to determine, whether the same D″ structure can produce both PKP precursors and D″ reflections. For this we use AxiSEM, an axisymmetric spectral element method (Nissen-Meyer et al., 2014). The principle of AxiSEM is to rotate a 1-D Earth model around an axis going through the source and the Earth's center, resulting in a 2.5-D model which is used to compute the Green's functions for a single force. The synthetic seismogram for a specific source and receiver can then be extracted from the Green's function database with Instaseis (van Driel et al., 2015). In our application we used a modified form of the isotropic PREM model (Dziewonski &

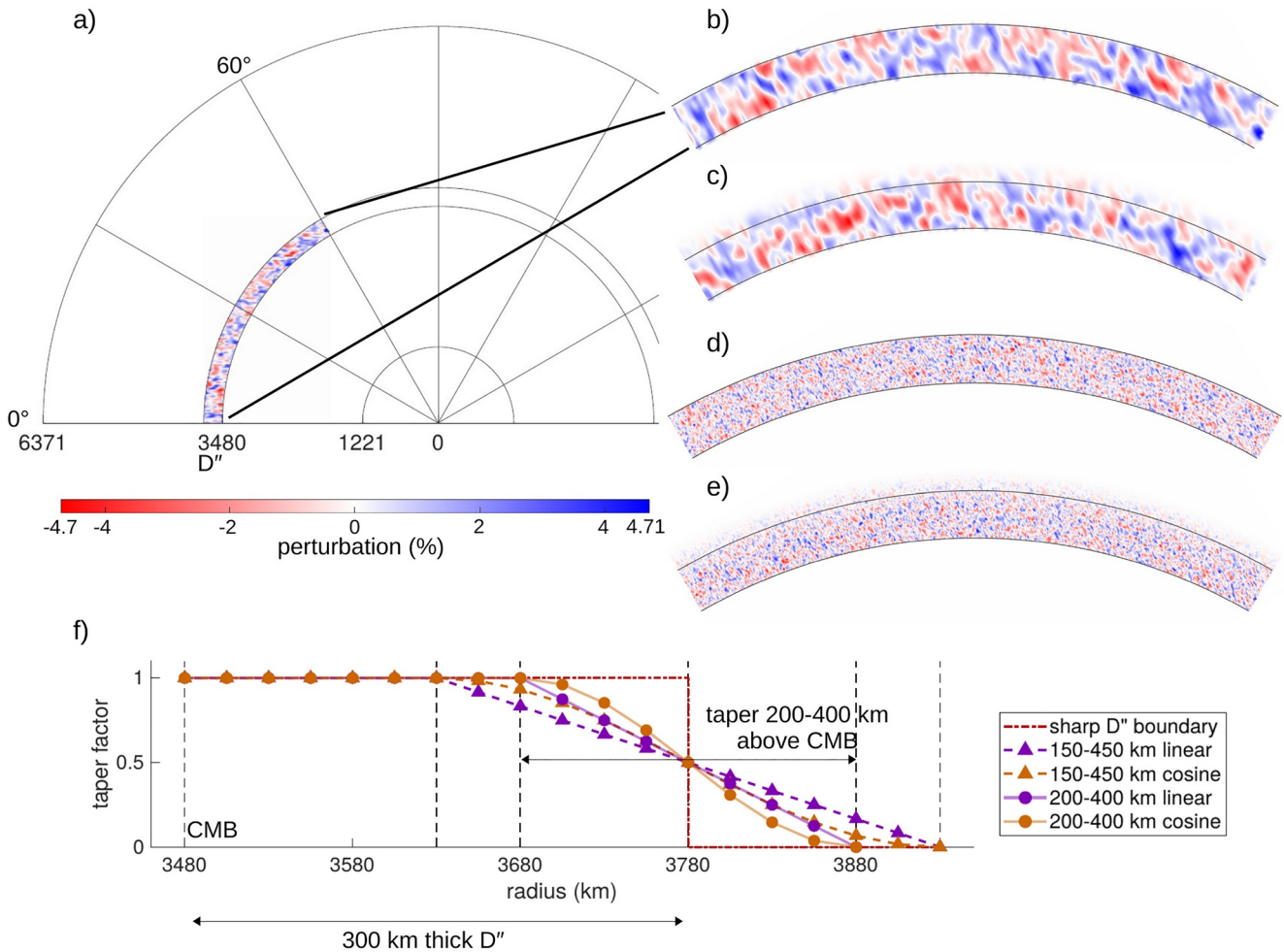

Figure 3. Random heterogeneity models of scatterers within the D″ region. (a) The heterogeneity model inserted in the D″ region. The scattering area has an average thickness of 300 km and is placed at the colatitude range of 0°–60° with the source location at 0° ensuring scattering for PKP precursors at the source side only. Panels (b)–(e) show different models: (b) Correlation length (corr) = 50 km, velocity perturbation (pert) = 5%. (c) Corr = 50 km, pert = 5%, with a cosine taper from 150 to 450 km above CMB. (d) Corr = 10 km, pert = 5%. (e) Corr = 10 km, pert = 5%, with a cosine taper from 150 to 450 km above CMB. (f) Linear (purple) and cosine (orange) tapers of different widths around the upper D″ boundary applied to the heterogeneity model to ensure a smooth onset of scattering compared with the sharp D″ boundary (red dashed line).

Anderson, 1981), that is, PREM light, as implemented in AxiSEM, as the reference model. The parameters in AxiSEM are set to their default values (AxiSEM's user manual, Nissen-Meyer et al., 2014) except for the dominant period which we set as 2 s, and the viscoelastic attenuation which is turned off since the included attenuation model was not suitable enough for our small-scale scattering, resulting in a loss of shorter periods. Therefore, important phase information of especially the PdP reflections but also in the PKP precursors would vanish in our considered period ranges (Figure S2 in Supporting Information S1).

In the reference model, we replaced a defined region at the CMB by a heterogeneity model (Figure 3), situated at the co-latitude range of 0°–60° (see Figure 3a) with the source at 0° leading to a source-side model for the PKP precursors. This setup ensures that scattering of PKP waves occurs only at the source side and not at the exit from the core at the receiver side. The heterogeneity model consists of randomly distributed scatterers in the D″ layer with different correlation lengths and relative perturbation values. For the correlation lengths we chose 10 and 50 km, and for the perturbation values 1%, 3%, and 5%. Furthermore, we varied the sharpness of the heterogeneity boundary at the top by putting a taper of different shape and width at the edge of the region (see Figures 3b–3f). A sudden onset of a scattering region would always generate reflections; therefore, we soften the transition to test whether a smoothly increasing scattering region still explains our observations. The taper was only applied

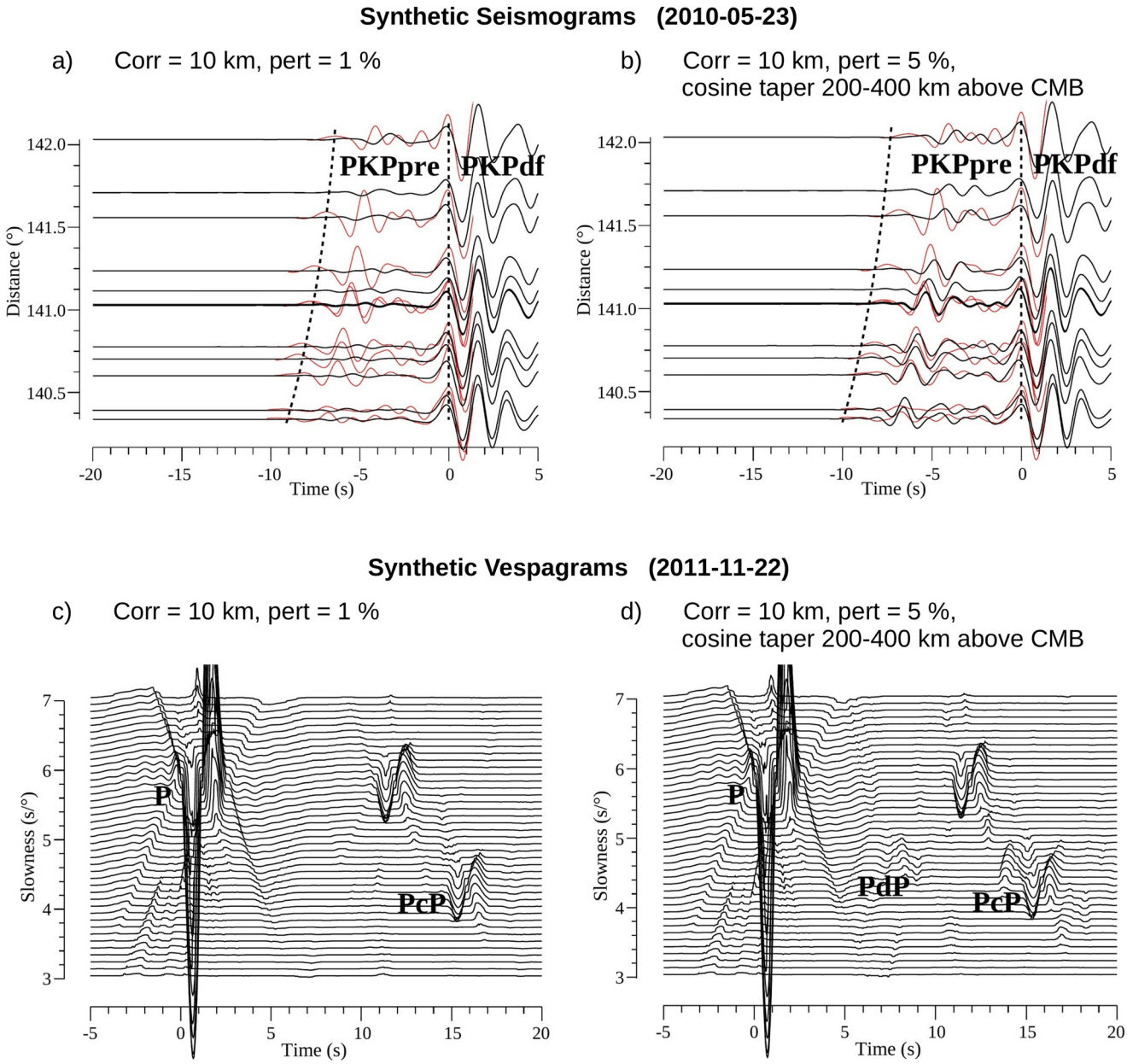

Figure 4. (a)–(b) Synthetic precursor data of event 23 May 2010, bandpass filtered with corner periods of 1–3 s, and aligned on PKPdf for two different scattering models: (a) Corr = 10 km, pert = 1%. (b) Corr = 10 km, pert = 5%, including a cosine taper 200–400 km above the CMB. The red lines show the real data traces, while the black traces are for the synthetic data (there were no data for two stations at the time of the event). (c)–(d) Vespagrams of synthetic data for event 22 November 2011, bandpass filtered with corner periods of 1–10 s. (c) Corr = 10 km, pert = 1%. (d) Corr = 10 km, pert = 5%, including a cosine taper 200–400 km above CMB. The arrival that could be interpreted as D″ reflection is marked with PdP. The arrival in both figures with P-slowness is the Moho-multiple.

for perturbations of 3% and 5%, due to already very weak precursor and reflection signals from a 1% velocity variation, which were reduced even further with a taper.

The synthetic seismograms of various heterogeneity models were computed for the events in Figures 2a and 2c. Comparing the precursor data (Figures 4a and 4b), the model that generates synthetics most similar to the event in Figure 2a has a correlation length of 10 km, a perturbation of 5% and a cosine-taper from 200 to 400 km above the CMB (Figure 4b). For this we visually inspected the waveforms of three stations with different distances and compared them to the corresponding traces of the real data. The model that led to the most similar waveforms was defined as the best fitting model. In Figures 4a and 4b, the comparison is shown for all traces in the period

range 1–3 s. Also using another random model with the same best fitting parameters (imitated by a slight shift of the receivers) lead to similar waveforms. Using a correlation length of 10 km and a perturbation of 1%, precursors to PKP are still visible, but much weaker than when using a stronger perturbation (Figure 4a). The greater the correlation length and perturbation, the greater are the precursors amplitudes, which leads to a stronger scattering (compare also Table S3 in Supporting Information S1). Observations of scattering in the Earth also show a large range of amplitudes and therefore a range of perturbations and correlation lengths may explain published observations (e.g., Mancinelli et al., 2016; Ma & Thomas, 2020; Thomas et al., 1999; Waszek et al., 2015).

For the models used above we used traces in the distance range of the D″ reflection event in Figure 2c and produced vespagrams. Here, we focused on the question whether our models can produce any waves that would be identified as PdP reflections, rather than expecting that the model matches the reflection data perfectly. We found that small correlation lengths and perturbations create only very weak signals or no visible PdP arrivals (Figure 4c, Table S4 in Supporting Information S1). However, our best fitting model for PKP precursors also produces clearly visible PdP waves in the vespagram (Figure 4d), interestingly with a polarity that seems to be opposite that of PcP which has also been observed in previous studies (e.g., Cobden & Thomas, 2013; Pisconti et al., 2019; Thomas et al., 2011). The corresponding traces for this model are shown in Figure S1b in Supporting Information S1 and a small coherent arrival is visible between P and PcP (marked as PdP). In other cases, we find PdP reflections from our scattering models that have the same polarity as PcP waves. Furthermore, we find that PdP waves were also observed for different tapers used to flatten the scattering boundary (as for example the cosine-taper from 200 to 400 km above the CMB used in Figure 4d) therefore we assume that the reflection is not generated by the onset of scattering. We also compared our random scattering model to a layered heterogeneity (i.e., including a D″ discontinuity) and found that a higher velocity variation is needed in a scattering model to produce similar PdP reflections (Figure S3 in Supporting Information S1). In addition, we tested with our best fitting model for precursors whether SdS-like waves in the T-component are generated and found a small wave that we would identify as SdS phase similar to the PdP in Figure 4d.

4. Discussion

In previous works, Haddon and Cleary (1974) explained observed PKP precursors amplitudes by a scattering medium with a correlation length of 30 km and a velocity variation of 1%, while Bataille and Flatté (1988) inferred a similar velocity perturbation of 0.5%–1%. Instead, Cormier (1995), Wen (2000), and Niu and Wen (2001) found that a velocity perturbation of up to 10% in the D″ layer fit their data better than smaller perturbation, and finally Vidale and Hedlin (1998) found a velocity perturbation of 13% and a scale length of 10 km in a thin (i.e., 60 km) layer at the CMB. In contrast, the velocity variation of whole-mantle scattering ranges from 0.1% to 1% (e.g., Cormier, 1999; Mancinelli & Shearer, 2013; Margerin & Nolet, 2003).

Our models encompass the D″ region with an average thickness of 300 km and our scattering heterogeneities were modeled with parameters in the range of 10 and 50 km and 3% and 5%. The best fitting model with a velocity perturbation of 5% and a scale-length of 10 km is similar to the previously published parameters. However, there is a highly variable range of the velocity variation in previous studies, which depend also on the depth distribution of the scattering layer or on the location. Interestingly, our precursor amplitudes and timing of our best fitting model shows a coherent precursor signal (similar to e.g., Ma & Thomas, 2020) and also agrees with a similar arrival in the real data (Figure 2a). Such coherent precursors have also been modeled with ULVZs embedded in a scattering regime (Ma & Thomas, 2020). The synthetic seismogram of a weak scattering model (Figure 4a) on the other hand, agrees with the PKP precursor amplitudes in the event shown in Figure 2b. Detailed relations of the model parameters as correlation length, perturbation and taper to the variability in PKP precursor amplitudes and frequencies will be investigated in a follow-up study.

The dimensions of our scattering heterogeneity are similar to previous studies as explained above. In those studies, small-scale scatterers were related, among others, to ULVZs (e.g., Jackson & Thomas, 2021; Ma et al., 2019; Ma & Thomas, 2020; Thomas et al., 1999). These seismic observations of ULVZs were explained by an iron-rich post-perovskite model (Mao et al. (2006). On the other hand, Haugland et al. (2018) explained PKP scattering with a model including mid-ocean ridge basalt (MORB). Also melt pockets have been suggested as cause for small-scale scatterers (e.g., Hedlin & Shearer, 2000). As our scattering model is similar to those published and

interpreted before, here we cannot differentiate between different causes for small-scale heterogeneity and more work is needed to identify the cause of scattering in the lowermost mantle.

Since we test the hypothesis that the same structure in D″ can generate different seismic observations when tested with either different waves or methods, we find that our scattering model can also generate signals that would be interpreted as D″ reflections. In some of the vespagrams a wave appears with the correct slowness and timing for such a reflection (Table S4 in Supporting Information S1). However, several of the vespagrams also show different arrivals that would usually be ignored due to the different slowness values compared with expected PdP slowness. In seismic data, PdP reflections appear highly variable in many studies (e.g., Cobden et al., 2015; Jackson & Thomas, 2021; Wysession et al., 1998), displaying different travel times and often different waveforms caused by for example, changes in the reflector depth, anisotropy or velocity gradient. Previous studies have also reported two or more reflectors (e.g., Lay et al., 2006; Thomas, Garnero, & Lay, 2004) that have been interpreted as reflection at the phase transition to post-perovskite and further down back to bridgmanite (e.g., Hernlund et al., 2005) or as due to a phase transition in mid-ocean ridge basalt and an ULVZ (e.g., Lay et al., 2006; Ohta et al., 2008). Our models generate the same behavior as seen for D″ reflections: We find variable amplitudes, slowness values and timing as well as polarity variations of our signals that can be interpreted as D″ reflection (Table S4 in Supporting Information S1). PdP polarities have been discussed in the context of anisotropy before (Pisconti et al., 2019) and we cannot exclude this possibility here. However, scattering would probably generate strongly variable polarities over short distances, while anisotropy may generate more homogeneous polarity observations. Anisotropic scattering as tested by Mancinelli et al. (2016) may also generate more coherent polarity observations for PdP reflections but this case is not included in our study.

In our reflection data generated with the scattering model, many events show additional signals in the time window between P and PcP (e.g., Figure 2c) similar to events shown, for example, in Thomas, Garnero and Lay (2004), Thomas, Kendall and Lowman (2004) and Chaloner et al. (2009), which could be interpreted as double crossing signal (Hernlund et al., 2005) or noise contamination. In summary, our results provide an additional explanation for the strong variation in D″ reflection data even within one region and could also help to explain D″ reflections within low velocity regions.

This is, however, not the first time that scattering has been invoked to explain signals between P and PcP: previous studies by Scherbaum et al. (1997) and Braña and Helffrich (2004) have already suggested that localized scatterers could be responsible for intermittent D″ reflection observations and our analysis shows that not only localized scatterers as suggested by Scherbaum et al. (1997) and Braña and Helffrich (2004) are generating the D″ reflection but that also a random scattering medium generates D″ reflection-like arrivals. Since the velocity perturbation and correlation length have an effect on amplitude of both the PKP precursor waves and the D″ reflection data, a comparison of scattering amplitudes and PdP or SdS waves in the same areas could help to verify that both waves are caused by the same mechanism. In our region beneath the Central Atlantic, the best fitting model can explain both observations, however, the sampling region is not in exactly the same spot.

5. Conclusion

In this study, we test the hypothesis that a scattering medium can generate PKP precursor data and arrivals that could be interpreted as D″ reflections. Since many structures in D″ are interrogated with different waves, epicentral distances and frequencies, the connection between these structures are currently not clear. Using available source-array combinations, it is difficult to test one region with a number of waves and methods, but we find one region that shows both scattering and PdP reflections in real data albeit not exactly in the same place. To test our assumption, we computed synthetic data for selected events where we could observe either strong PKP precursors in real data, or D″ reflections in P-wave data. The models implemented at the CMB are composed of a scattering medium with different correlation lengths and velocity perturbation values. Our best fitting model for generating PKP precursor consists of a correlation length of 10 km, a velocity perturbation of 5% and a cosine-taper from 200 to 400 km above the CMB which avoids the sudden onset of scattering. This model also produced a wave that we would usually identify as PdP. Our modeling shows variations in amplitudes, slowness, timing of arrivals, polarities of waves and waveforms as seen in real data for PKP precursors and PdP waves. This suggests that variations in observed data could potentially be explained by scattering regions with variable velocity perturbation and correlation lengths. Studying one region with a range of different waves such as diffracted

or converted waves could determine whether structures in D″ are related to each other and whether strongly variable interpretations of D″ structure are due to missing information, since many studies are only restricted to one wavetype and method.

Data Availability Statement

Data were downloaded from the Incorporated Research Institute for Seismology (IRIS) and used from the 3D array (https://doi.org/10.7914/SN/3D_2010) and KN array (https://doi.org/10.7914/SN/KN). Maps were drawn with GMT (Wessel and Smith, 1995) and data were analyzed with Seismic Handler (Stammler, 1993). The software AxiSEM (https://geodynamics.org/cig/software/axisem/) and Instaseis (https://instaseis.net/) are freely available.

Acknowledgments
The authors would like to thank the editor Daoyuan Sun, the reviewer Daniel A. Frost and an anonymous reviewer for their helpful comments and suggestions which greatly improved the manuscript. The project was partly supported by TH1530/18-1. Open access funding enabled and organized by Projekt DEAL.

References

Ansell, J. H. (1973). Precursors to PKP: Seismic wave scattering and spectral data. *Geophysical Journal International*, *35*(4), 487–489. https://doi.org/10.1111/j.1365-246X.1973.tb00610.x

Avants, M., Lay, T., Russell, S. A., & Garnero, E. J. (2006). Shear velocity variations within the D″ region beneath the central Pacific. *Journal of Geophysical Research*, *111*, B05305. https://doi.org/10.1029/2004JB003270

Bataille, K., & Flatté, S. M. (1988). Inhomogeneities near the core-mantle boundary inferred from short-period scattered PKP waves recorded at the global Digital Seismograph Network. *Journal of Geophysical Research*, *93*(B12), 15057–15064. https://doi.org/10.1029/JB093iB12p15057

Bataille, K., Wu, R.-S., & Flatté, S. M. (1990). Inhomogeneities near the core-mantle boundary evidenced from scattered waves: A review. *Pure and Applied Geophysics*, *132*(1–2), 151–173. https://doi.org/10.1007/BF00874361

Bower, D. J., Gurnis, M., & Sun, D. (2013). Dynamic origins of seismic wavespeed variation in D. *Physics of the Earth and Planetary Interiors*, *214*, 74–86. https://doi.org/10.1016/j.pepi.2012.10.004

Braña, L., & Helffrich, G. (2004). A scattering region near the core-mantle boundary under the North Atlantic. *Geophysical Journal International*, *158*(2), 625–636. https://doi.org/10.1111/j.1365-246X.2004.02306.x

Bullen, K. E. (1949). Compressibility-pressure hypothesis and the Earth's interior. *Geophysical Supplement to the Monthly Notices of the Royal Astronomical Society*, *5*(9), 335–368. https://doi.org/10.1111/j.1365-246X.1949.tb02952.x

Cao, A., & Romanowicz, B. (2007). Locating scatterers in the mantle using array analysis of PKP precursors from an earthquake doublet. *Earth and Planetary Science Letters*, *255*(1–2), 22–31. https://doi.org/10.1016/j.epsl.2006.12.002

Chaloner, J. W., Thomas, C., & Rietbrock, A. (2009). P- and S-wave reflectors in D″ beneath southeast Asia. *Geophysical Journal International*, *179*(2), 1080–1092. https://doi.org/10.1111/j.1365-246X.2009.04328.x

Cleary, J. R., & Haddon, R. A. W. (1972). Seismic wave scattering near the core-mantle boundary: A new interpretation of precursors to PKP. *Nature*, *240*, 549–551. https://doi.org/10.1038/240549a0. https://doi.org/10.1038/240549a0

Cobden, L., & Thomas, C. (2013). The origin of D″ reflections: A systematic study of seismic array data sets. *Geophysical Journal International*, *194*(2), 1091–1118. https://doi.org/10.1093/gji/ggt152

Cobden, L., Thomas, C., & Trampert, J. (2015). Seismic detection of post-perovskite inside the Earth. In A. Khan, & F. Deschamps (Eds.), *The Earth's heterogeneous mantle* (pp. 391–440). Springer. https://doi.org/10.1007/978-3-319-15627-9_13

Cormier, V. F. (1995). Time-domain modelling of PKIKP precursors for constraints on the heterogeneity in the lowermost mantle. *Geophysical Journal International*, *121*(3), 725–736. https://doi.org/10.1111/j.1365-246X.1995.tb06434.x

Cormier, V. F. (1999). Anisotropy of heterogeneity scale lengths in the lower mantle from PKIKP precursors. *Geophysical Journal International*, *136*(2), 373–384. https://doi.org/10.1046/j.1365-246X.1999.00736.x

Davies, G. F., & Gurnis, M. (1986). Interaction of mantle dregs with convection: Lateral heterogeneity at the core-mantle boundary. *Geophysical Research Letters*, *13*(13), 1517–1520. https://doi.org/10.1029/GL013i013p01517

Doornbos, D. J. (1976). Characteristics of lower mantle inhomogeneities from scattered waves. *Geophysical Journal International*, *44*(2), 447–470. https://doi.org/10.1111/j.1365-246X.1976.tb03667.x

Doornbos, D. J., & Vlaar, N. J. (1973). Regions of seismic wave scattering in the Earth's mantle and precursors to PKP. *Nature; Physical Science*, *243*, 58–61. https://doi.org/10.1038/physci243058a0

Dziewonski, A. M., & Anderson, D. L. (1981). Preliminary reference Earth model. *Physics of the Earth and Planetary Interiors*, *25*(4), 297–356. https://doi.org/10.1016/0031-9201(81)90046-7

French, S. W., & Romanowicz, B. (2015). Broad plumes rooted at the base of the Earth's mantle beneath major hotspots. *Nature*, *525*, 95–99. https://doi.org/10.1038/nature14876

Garnero, E. J., McNamara, A. K., & Shim, S.-H. (2016). Continent-sized anomalous zones with low seismic velocity at the base of Earth's mantle. *Nature Geoscience*, *9*, 481–489. https://doi.org/10.1038/ngeo2733

Garnero, E. J., Revenaugh, J., Williams, Q., Lay, T., & Kellogg, L. H. (1998). Ultralow velocity zone at the core-mantle boundary. In M. Gurnis, M. E. Wysession, E. Knittle, & B. A. Buffett (Eds.), *The Core-Mantle Boundary Region* (Vol. 28, pp. 319–334). American Geophysical Union. https://doi.org/10.1029/gd028p0319

Gutenberg, B., & Richter, C. F. (1934). On seismic waves (first paper). *Gerlands Beiträge zur Geophysik*, *43*, 56–133.

Haddon, R. A. W. (1972). Corrugations on the mantle-core boundary or transition layers between inner and outer cores? *Eos, Transactions of the American Geophysical Union*, *53*, 600.

Haddon, R. A. W., & Cleary, J. R. (1974). Evidence for scattering of seismic PKP waves near the mantle-core boundary. *Physics of the Earth and Planetary Interiors*, *8*(3), 211–234. https://doi.org/10.1016/0031-9201(74)90088-0

Haugland, S. M., Ritsema, J., van Keken, P. E., & Nissen-Meyer, T. (2018). Analysis of PKP scattering using mantle mixing simulations and axisymmetric 3D waveforms. *Physics of the Earth and Planetary Interiors*, *276*, 226–233. https://doi.org/10.1016/j.pepi.2017.04.001

Hedlin, M. A. H., & Shearer, P. M. (2000). An analysis of large-scale variations in small-scale mantle heterogeneity using Global Seismographic Network recordings of precursors to PKP. *Journal of Geophysical Research*, *105*(B6), 13655–13673. https://doi.org/10.1029/2000JB900019

Hedlin, M. A. H., Shearer, P. M., & Earle, P. S. (1997). Seismic evidence for small-scale heterogeneity throughout the Earth's mantle. *Nature*, *387*, 145–150. https://doi.org/10.1038/387145a0

Hernlund, J. W., Thomas, C., & Tackley, P. J. (2005). A doubling of the post-perovskite phase boundary and structure of the Earth's lowermost mantle. *Nature*, *434*, 882–886. https://doi.org/10.1038/nature03472

Houard, S., & Nataf, H.-C. (1993). Laterally varying reflector at the top of beneath Northern Siberia. *Geophysical Journal International*, *115*(1), 168–182. https://doi.org/10.1111/j.1365-246X.1993.tb05597.x

Hutko, A. R., Lay, T., Garnero, E. J., & Revenaugh, J. (2006). Seismic detection of folded, subducted lithosphere at the core-mantle boundary. *Nature*, *441*, 333–336. https://doi.org/10.1038/nature04757

Hutko, A. R., Lay, T., Revenaugh, J., & Garnero, E. J. (2008). Anticorrelated seismic velocity anomalies from post-perovskite in the lowermost mantle. *Science*, *320*(5879), 1070–1074. https://doi.org/10.1126/science.1155822

Jackson, J. M., & Thomas, C. (2021). Seismic and mineral physics constraints on the D″ layer. In H. Marquardt, M. Ballmer, S. Cottaar, & J. Konter (Eds.), *Mantle Convection and Surface Expressions* (Vol. 263, pp. 193–227). American Geophysical Union, John Wiley & Sons, Inc. https://doi.org/10.1002/9781119528609.ch8

Kendall, J.-M. (2000). Seismic anisotropy in the boundary layers of the mantle. In S.-I. Karato, A. Forte, R. Liebermann, G. Masters, & L. Stixrude (Eds.), *Earth's Deep Interior: Mineral Physics and Tomography From the Atomic to the Global Scale* (Vol. 117, pp. 133–159). American Geophysical Union. https://doi.org/10.1029/gm117p0133

King, D. W., Haddon, R. A. W., & Cleary, J. R. (1974). Array analysis of precursors to PKIKP in the distance range 128° to 142°. *Geophysical Journal International*, *37*(1), 157–173. https://doi.org/10.1111/j.1365-246X.1974.tb02450.x

Koelemeijer, P. (2021). Toward consistent seismological models of the core-mantle boundary landscape. In H. Marquardt, M. Ballmer, S. Cottaar, & J. Konter (Eds.), *Mantle Convection and Surface Expressions* (Vol. 263, pp. 229–255). American Geophysical Union, John Wiley & Sons, Inc. https://doi.org/10.1002/9781119528609.ch9

Lay, T. (2015). Deep Earth structure: Lower mantle and D. In G. Schubert (Ed.), *Treatise on geophysics* (2nd ed., pp. 683–723). Elsevier. Chap. 1.22. https://doi.org/10.1016/B978-0-444-53802-4.00019-1

Lay, T., & Garnero, E. J. (2004). Core-mantle boundary structures and processes. In R. S. J. Sparks, & C. J. Hawkesworth (Eds.), *The State of the Planet: Frontiers and Challenges in Geophysics* (Vol. 150, pp. 25–41). American Geophysical Union. https://doi.org/10.1029/150gm04

Lay, T., Garnero, E. J., Young, C. J., & Gaherty, J. B. (1997). Scale lengths of shear velocity heterogeneity at the base of the mantle from S wave differential travel times. *Journal of Geophysical Research*, *102*(B5), 9887–9909. https://doi.org/10.1029/97JB00331

Lay, T., & Helmberger, D. V. (1983). A lower mantle S-wave triplication and the shear velocity structure of D. *Geophysical Journal International*, *75*(3), 799–837. https://doi.org/10.1111/j.1365-246X.1983.tb05010.x

Lay, T., Hernlund, J., Garnero, E. J., & Thorne, M. S. (2006). A post-perovskite lens and D″ heat flux beneath the central Pacific. *Science*, *314*(5803), 1272–1276. https://doi.org/10.1126/science.1133280

Lay, T., Williams, Q., & Garnero, E. J. (1998). The core-mantle boundary layer and deep Earth dynamics. *Nature*, *392*, 461–468. https://doi.org/10.1038/33083

Ma, X., Sun, X., & Thomas, C. (2019). Localized ultra-low velocity zones at the eastern boundary of Pacific LLSVP. *Earth and Planetary Science Letters*, *507*, 40–49. https://doi.org/10.1016/j.epsl.2018.11.037

Ma, X., & Thomas, C. (2020). Small-scale scattering heterogeneities in the lowermost mantle from a global analysis of PKP precursors. *Journal of Geophysical Research: Solid Earth*, *125*(3), e2019JB018736. https://doi.org/10.1029/2019JB018736

Mancinelli, N., Shearer, P., & Thomas, C. (2016). On the frequency dependence and spatial coherence of PKP precursor amplitudes. *Journal of Geophysical Research: Solid Earth*, *121*(3), 1873–1889. https://doi.org/10.1002/2015JB012768

Mancinelli, N. J., & Shearer, P. M. (2013). Reconciling discrepancies among estimates of small-scale mantle heterogeneity from PKP precursors. *Geophysical Journal International*, *195*(3), 1721–1729. https://doi.org/10.1093/gji/ggt319

Mao, W. L., Mao, H.-K., Sturhahn, W., Zhao, J., Prakapenka, V. B., Meng, Y., et al. (2006). Iron-rich post-perovskite and the origin of ultralow-velocity zones. *Science*, *312*(5773), 564–565. https://doi.org/10.1126/science.1123442

Margerin, L., & Nolet, G. (2003). Multiple scattering of high-frequency seismic waves in the deep Earth: PKP precursor analysis and inversion for mantle granularity. *Journal of Geophysical Research*, *108*(B11), 2514. https://doi.org/10.1029/2003JB002455

Maupin, V. (1994). On the possibility of anisotropy in the D″ layer as inferred from the polarization of diffracted S waves. *Physics of the Earth and Planetary Interiors*, *87*(1–2), 1–32. https://doi.org/10.1016/0031-9201(94)90019-1

McNamara, A. K. (2019). A review of large low shear velocity provinces and ultra low velocity zones. *Tectonophysics*, *760*, 199–220. https://doi.org/10.1016/j.tecto.2018.04.015

McNamara, A. K., Garnero, E. J., & Rost, S. (2010). Tracking deep mantle reservoirs with ultra-low velocity zones. *Earth and Planetary Science Letters*, *299*(1–2), 1–9. https://doi.org/10.1016/j.epsl.2010.07.042

Mellors, R. J. (1995). *Two studies in Central Asian seismology: A teleseismic study of the Pamir/Hindu Kush seismic zone and analysis of data from the Kyrgyzstan broadband seismic network. PhD thesis*. Indiana University.

Nissen-Meyer, T., van Driel, M., Stähler, S. C., Hosseini, K., Hempel, S., Auer, L., et al. (2014). AxiSEM: Broadband 3-D seismic wavefields in axisymmetric media. *Solid Earth*, *5*(1), 425–445. https://doi.org/10.5194/se-5-425-2014

Niu, F., & Wen, L. (2001). Strong seismic scatterers near the core-mantle boundary west of Mexico. *Geophysical Research Letters*, *28*(18), 3557–3560. https://doi.org/10.1029/2001GL013270

Nowacki, A., Wookey, J., & Kendall, J.-M. (2011). New advances in using seismic anisotropy, mineral physics and geodynamics to understand deformation in the lowermost mantle. *Journal of Geodynamics*, *52*(3–4), 205–228. https://doi.org/10.1016/j.jog.2011.04.003

Ohta, K., Hirose, K., Lay, T., Sata, N., & Ohishi, Y. (2008). Phase transitions in pyrolite and MORB at lowermost mantle conditions: Implications for a MORB-rich pile above the core-mantle boundary. *Earth and Planetary Science Letters*, *267*(1–2), 107–117. https://doi.org/10.1016/j.epsl.2007.11.037

Pisconti, A., Thomas, C., & Wookey, J. (2019). Discriminating between causes of D″ anisotropy using reflections and splitting measurements for a single path. *Journal of Geophysical Research: Solid Earth*, *124*(5), 4811–4830. https://doi.org/10.1029/2018JB016993

Reasoner, C., & Revenaugh, J. (1999). Short-period P wave constraints on D″ reflectivity. *Journal of Geophysical Research*, *104*(B1), 955–961. https://doi.org/10.1029/1998JB900053

Ritsema, J., Deuss, A., van Heijst, H. J., & Woodhouse, J. H. (2011). S40RTS: A degree-40 shear-velocity model for the mantle from new Rayleigh wave dispersion, teleseismic traveltime and normal-mode splitting function measurements. *Geophysical Journal International*, *184*(3), 1223–1236. https://doi.org/10.1111/j.1365-246X.2010.04884.x

Rost, S., Garnero, E. J., Williams, Q., & Manga, M. (2005). Seismological constraints on a possible plume root at the core-mantle boundary. *Nature*, *435*, 666–669. https://doi.org/10.1038/nature03620

Rost, S., & Thomas, C. (2002). Array seismology: Methods and applications. *Reviews of Geophysics*, *40*(3), 1008. https://doi.org/10.1029/2000RG000100

Scherbaum, F., Krüger, F., & Weber, M. (1997). Double beam imaging: Mapping lower mantle heterogeneities using combinations of source and receiver arrays. *Journal of Geophysical Research*, *102*(B1), 507–522. https://doi.org/10.1029/96JB03115

Schweitzer, J., Fyen, J., Mykkeltveit, S., Gibbons, S. J., Pirli, M., Kühn, D., & Kværna, T. P. (2012). Seismic arrays. In P. Bormann (Ed.), *New manual of seismological observatory practice (NMSOP-2)* (p. 1–80). *Potsdam: Deutsches GeoForschungszentrum GFZ* Chap. 9. https://doi.org/10.2312/GFZ.NMSOP-2_ch9

Sidorin, I., Gurnis, M., & Helmberger, D. V. (1999). Evidence for a ubiquitous seismic discontinuity at the base of the mantle. *Science*, *286*(5443), 1326–1331. https://doi.org/10.1126/science.286.5443.1326

Spieker, K., Wölbern, I., Thomas, C., Harnafi, M., & El Moudnib, L. (2014). Crustal and upper-mantle structure beneath the western Atlas Mountains in SW Morocco derived from receiver functions. *Geophysical Journal International*, *198*(3), 1474–1485. https://doi.org/10.1093/gji/ggu216

Stammler, K. (1993). Seismichandler – Programmable multichannel data handler for interactive and automatic processing of seismological analyses. *Computers & Geosciences*, *19*(2), 135–140. https://doi.org/10.1016/0098-3004(93)90110-Q

Sun, D., Helmberger, D., Miller, M. S., & Jackson, J. M. (2016). Major disruption of D″ beneath Alaska. *Journal of Geophysical Research: Solid Earth*, *121*(5), 3534–3556. https://doi.org/10.1002/2015JB012534

Thomas, C., Garnero, E. J., & Lay, T. (2004). High-resolution imaging of lowermost mantle structure under the Cocos plate. *Journal of Geophysical Research*, *109*, B08307. https://doi.org/10.1029/2004JB003013

Thomas, C., Kendall, J.-M., & Lowman, J. (2004). Lower-mantle seismic discontinuities and the thermal morphology of subducted slabs. *Earth and Planetary Science Letters*, *225*(1–2), 105–113. https://doi.org/10.1016/j.epsl.2004.05.038

Thomas, C., & Weber, M. (1997). P velocity heterogeneities in the lower mantle determined with the German regional seismic Network: Improvement of previous models and results of 2D modelling. *Physics of the Earth and Planetary Interiors*, *101*(1–2), 105–117. https://doi.org/10.1016/S0031-9201(96)03245-1

Thomas, C., Weber, M., Wicks, C. W., & Scherbaum, F. (1999). Small scatterers in the lower mantle observed at German broadband arrays. *Journal of Geophysical Research*, *104*(B7), 15073–15088. https://doi.org/10.1029/1999JB900128

Thomas, C., Wookey, J., Brodholt, J., & Fieseler, T. (2011). Anisotropy as cause for polarity reversals of D″ reflections. *Earth and Planetary Science Letters*, *307*(3–4), 369–376. https://doi.org/10.1016/j.epsl.2011.05.011

Thorne, M. S., Pachhai, S., Leng, K., Wicks, J. K., & Nissen-Meyer, T. (2020). New candidate ultralow-velocity zone locations from highly anomalous SpdKS waveforms. *Minerals*, *10*(3), 211. https://doi.org/10.3390/min10030211

van Driel, M., Krischer, L., Stähler, S. C., Hosseini, K., & Nissen-Meyer, T. (2015). Instaseis: Instant global seismograms based on a broadband waveform database. *Solid Earth*, *6*(2), 701–717. https://doi.org/10.5194/se-6-701-2015

Vanacore, E., Niu, F., & Ma, Y. (2010). Large angle reflection from a dipping structure recorded as a PKIKP precursor: Evidence for a low velocity zone at the core-mantle boundary beneath the Gulf of Mexico. *Earth and Planetary Science Letters*, *293*(1–2), 54–62. https://doi.org/10.1016/j.epsl.2010.02.018

Vernon, F. (1992). Kyrgyz seismic telemetry network. *IRIS Newsletter*, *XI*(1), 7–9.

Vernon, F. (1998). *Kyrgyz seismic network becomes cornerstone for new International Geodynamics Research Center* (p. 18). IRIS Newsletter XVII(2).

Vidale, J. E., & Hedlin, M. A. H. (1998). Evidence for partial melt at the core-mantle boundary north of Tonga from the strong scattering of seismic waves. *Nature*, *391*, 682–685. https://doi.org/10.1038/35601

Waszek, L., Thomas, C., & Deuss, A. (2015). PKP precursors: Implications for global scatterers. *Geophysical Research Letters*, *42*(10), 3829–3838. https://doi.org/10.1002/2015GL063869

Weber, M. (1993). P and S wave reflections from anomalies in the lowermost mantle. *Geophysical Journal International*, *115*(1), 183–210. https://doi.org/10.1111/j.1365-246X.1993.tb05598.x

Weber, M., & Davis, J. P. (1990). Evidence of a laterally variable lower mantle structure from P- and S-waves. *Geophysical Journal International*, *102*(1), 231–255. https://doi.org/10.1111/j.1365-246X.1990.tb00544.x

Weber, M., & Körnig, M. (1992). A search for anomalies in the lowermost mantle using seismic bulletins. *Physics of the Earth and Planetary Interiors*, *73*(1–2), 1–28. https://doi.org/10.1016/0031-9201(92)90104-4

Wen, L. (2000). Intense seismic scattering near the Earth's core-mantle boundary beneath the Comoros hotspot. *Geophysical Research Letters*, *27*(22), 3627–3630. https://doi.org/10.1029/2000GL011831

Wessel, P., & Smith, W. H. F. (1995). New version of the generic mapping tools released. *Eos, Transactions of the American Geophysical Union*, *76*(33), 329. https://doi.org/10.1029/95EO00198

Wright, C., Muirhead, K. J., & Dixon, A. E. (1985). The P wave velocity structure near the base of the mantle. *Journal of Geophysical Research*, *90*(B1), 623–634. https://doi.org/10.1029/JB090iB01p00623

Wysession, M. E., Lay, T., Revenaugh, J., Williams, Q., Garnero, E. J., Jeanloz, R., & Kellogg, L. H. (1998). The D″ discontinuity and its implications. In M. Gurnis, M. E. Wysession, E. Knittle, & B. A. Buffett (Eds.), *The Core-Mantle Boundary Region*, (Vol. 28, pp. 273–297). American Geophysical Union. https://doi.org/10.1029/gd028p0273